Reactive scattering of "hot" H atoms with CO_2 and OCS

Harry E. Cartland

Photonics Research Center, U.S. Military Academy
West Point, NY 10996

Scott L. Nickolaisen and Curt Wittig

Chemistry Department, University of Southern California
Los Angeles, CA 90089

ABSTRACT

Time-resolved infrared diode laser spectroscopy has been used to state selectively monitor CO produced in the "hot" atom reaction of H with CO_2 and OCS. For center of mass (CM) kinetic energies of 2.4 and 1.4 eV, respectively, CO internal excitations are substantially colder than predicted by statistical theory, with energy preferentially channeled into CM translation. In the collision energy regime of these experiments, $\approx$10,000 cm^{-1} above the barrier, statistical rate theory is not applicable even with an intermediate.

1. INTRODUCTION

Hydrogen atom reactions with CO_2 and OCS

$$H + CO_2 \rightarrow CO + OH \qquad \Delta H_{298} = 8960\ cm^{-1}$$

$$H + OCS \rightarrow CO + SH \qquad \Delta H_{298} = -3930\ cm^{-1}$$

are of interest because of their role in combustion and atmospheric chemistry. In addition, their relative simplicity makes them amenable to computational studies, allowing a rigorous comparison between experiment and current dynamical theories.

The two reactions present an interesting pair for comparison. Though the first is endothermic and the second exothermic, under the conditions employed here the barrier is crossed with $\approx$10,000 cm^{-1} of excess energy in both cases. As we shall see, both reactions yield qualitatively similar non-statistical CO product state distributions.

1.1. $H+CO_2 \rightarrow CO+OH$

The $H+CO_2$ reaction has already received considerable attention, mostly focussing on laser-induced fluorescence (LIF) detection of the OH fragment. Quick and Tiee detected OH in up to v=2 at a CM collision energy of 2.6 eV.[1] Kleinermanns et al. measured OH(v=0) rotational distributions for CM energies of 1.9 and 2.6 eV, and found them to be colder than statistical.[2] Jacobs et al. determined a reaction cross section of 0.4 ± 0.2 $Å^2$ at a collision energy of 1.9 eV.[3] Radhakrishnan et al.,[4] Rice et al.,[5] and Scherer et al.[6] have studied the reaction with complexed precursors, the last using a picosecond pump-probe technique to demonstrate the presence of an intermediate. Finally, Rice et al. have used VUV LIF to measure CO(v=0,1) rotational distributions under bulk and complexed conditions.[7] We consider the CO distributions of Rice et al., as well as the ab initio HOCO potential energy surface of Schatz et al.,[8] later in this paper.

 0-8194-0784-4/92/$4.00

1.2. $H+OCS \rightarrow CO+SH$

The $H+OCS$ reaction has also been studied previously, but not nearly to the same extent as $H+CO_2$. Tsunashina et al.[9] and Lee et al.[10] have measured the reaction rate constant, establishing an activation barrier of 1350 cm^{-1}. Using 193 nm photolysis of DBr as a D atom source, Hauesler et al. measured SD(v=0,1) rotational distributions under bulk and complexed conditions, and found them to be non-statistical;[11] predissociation prevents a similar analysis of the analogous H atom reaction. We return to the results of Hauesler et al. later in the discussion.

2. EXPERIMENTAL SECTION

The UV laser pump/IR diode laser probe technique has been described elsewhere in detail.[12] The apparatus used for the study of $H+CO_2$ was not the same as that used for $H+OCS$, but the differences were for the most part minor. We provide a general description of the technique, followed by a discussion of details specific to each experiment.

Translationally "hot" H atoms were generated in a 2 m pressure stabilized flow cell by a UV laser photolysis pulse. The pulse energy was measured during the course of the experiments to allow normalization of the measured nascent product distributions.

A collinear CW IR diode laser (Laser Analytics) then state selectively probed the CO(v,J) reaction product. The output of the IR diode was collimated and passed through a monochromator to select a single laser mode with a nominal linewidth of ≈ 0.0003 cm^{-1}. Because of anharmonicity, virtually any CO(v,J) level is accessible by temperature and current tuning of the diode output, though more than one diode is usually required to cover the wavelength range of interest. The distributions reported here are based on a sampling of even and odd J states in both the P and R branches.

Prior to entering the sample cell, $\approx 10\%$ of the IR beam was split off and passed through a reference flow cell. The reference cell and a Ge etalon permitted precise wavelength calibration. Passing a discharge through the cell generated a reference population in higher vibrational states (v>0), allowing excited product states to be probed in the sample cell.

Standard line locking techniques were used to prevent drift of the diode laser. The reference detector signal was input to a lock-in amplifier. By using phase sensitive detection, a small dither in the diode output produced an error signal which was fed back into the diode current controller to drive the laser output to line center.

The sample and reference beams passed through long wavepass filters ($\lambda > 2.5$ μm) before being focussed onto $N_2(\ell)$ cooled InSb detectors. The signal level was boosted by impedance matched preamplifiers and line drivers. The reference signal was input directly to the lock-in amplifier, while the sample signal underwent another stage of amplification and filtering prior to being input to a transient digitizer (LeCroy). The digitizer sampled the absorption transients at 10^8 samples s^{-1}, and hard wire averaged them in the CAMAC crate controller. The averaged data was stored, processed and displayed on a PC AT computer (IBM) using original software written in ASYST.

2.1. $H+CO_2 \rightarrow CO+OH$

Excimer laser (Lambda Physik) photolysis of H_2S at 193 nm produced H atoms with a CM kinetic energy of 2.4 eV (19,200 cm^{-1}). Although 193 nm photolysis actually produces H atoms with a distribution of kinetic energies corresponding to varying internal excitation of the SH fragment, the strong dependence of reaction probability on CM collision energy means that 96% of the reactive H atoms have this energy.[12a]

For this experiment, the sample mixture was 20% H_2S in CO_2 at a total pressure of 200 mTorr. Typically 1500 transient signals were averaged at a repetition rate of 10 Hz. Detection system response time was 200 μs.

2.2. H+OCS → CO+OH

Hydrogen atoms were generated by 278 nm photolysis of HI. The 278 nm photons were produced by doubling the output of a Nd:YAG pumped dye laser (Quantel) using Rhodamine 590 dye. Pulse energies were typically 10-12 mJ. At this wavelength, 90% of the I atoms are produced in the $^2P_{1/2}$ ground state,[13] yielding a H atom CM energy of 1.4 eV (11,100 cm^{-1}).

Normally 250 transient signals were averaged at a repetition rate of 2 Hz. The sample mixture was 20% HI in OCS with both components requiring distillation before use. Sample pressure was typically 200 or 400 mTorr, but ranged from 50 to 1000 mTorr during pressure studies. Using a photodissociation process that produced CO, the detection system risetime was measured at $\approx$80 ns.

For time-resolved CO(v,J) lineshape measurements, a fraction of the IR beam was directed to a vacuum spaced confocal etalon (Laser Analytics). Instead of dithering the diode laser wavelength, the etalon scanner driver was modulated thereby dithering the fringe positions in time. The line locking technique described above was used to slave the laser output to an etalon fringe, which was subsequently stepped across the absorption feature of interest. Simultaneous acquisition of a room temperature CO reference lineshape served to calibrate the step size in terms of wavelength.

3. RESULTS

The raw data were converted to absorbance units by subtracting the AC coupled signal from the DC background, dividing the difference by the background, and taking the natural logarithm. Some typical v=0 signals from the H+OCS reaction are shown in Fig. 1. These transient signals clearly illustrate the reaction and CO relaxation dynamics. The two component rise for low J is evidence of a small nascent population, increased by rotational relaxation, and to a lesser extent vibrational relaxation, as equilibrium is reached. In contrast, high J levels show substantial initial populations which rapidly decay. Relaxation of a large nascent population to some non-zero value as thermal equilibrium is established is characteristic of intermediate J.

In order to interpret the data, we develop the following simple model where X designates either a O or S atom (X=O,S).

$$H^* + M \rightarrow H + M \qquad (1)$$

$$H^* + OCX \rightarrow CO(v,J) + XH \qquad (2)$$

$$H^* + OCX \rightarrow CO(v',J') + XH \qquad (2')$$

$$CO(v,J) + M \rightarrow CO(v',J') + M \qquad (3)$$

$$CO(v',J') + M \rightarrow CO(v,J) + M \qquad (3')$$

Reaction 1 is collisional deactivation, but effectively includes all processes that remove translationally "hot" H atoms, such as diffusion out of the probed volume and various radical reactions. Reactions 2 and 2' represent reactive scattering into the monitored state CO(v,J), and all other states CO(v',J'). Modelling the CO manifold as a quasi two level system consisting of the probed state and a "bath" state, with which energy is exchanged via reactions 3 and 3', yields an analytic expression for the time dependent CO(v,J) population [CO(v,J,t)]. As the fits in Fig. 1 show, the transient absorption signals are well modelled by this simple scheme.

The derivation of the analytic expression for [CO(v,J,t)], in various forms, is discussed elsewhere in detail.[12] Here we consider only two limiting cases. First, in the long time limit we find

$$[CO(v,J,t)]_{t\to\infty} = [H_o^*] \frac{(k_2\chi_{OCX}+k_{2'}\chi_{OCX})}{(k_1+k_2\chi_{OCX}+k_{2'}\chi_{OCX})} \frac{k_{3'}}{k_3+k_{3'}}$$

where $[H_o^*]$ is the initial "hot" H atom number density and χ_{OCX} is the mole fraction of the OCX (X=O,S) collision partner. This expression has a straight forward interpretation: the concentration of CO(v,J) after attainment of equilibrium is a product of the initial "hot" H atom concentration, the branching ratio for reactive scattering, and the equilibrium fraction of molecules in that state. Of more interest, though, is the short time limit

$$[CO(v,J,t)]_{t\to 0} = k_2\chi_{OCX}[H_o^*]\,[M]\,t$$

where [M] is the total sample number density. Initially, the CO(v,J) density is linear in time, with a proportionality constant dependent on the state specific rate constant k_2. Therefore, a plot of the initial slopes of the transient signals gives a relative distribution of state specific rates, which is equivalent to plotting the actual nascent CO(v,J) number densities.

Confidence in the distributions obtained in this manner requires that the model incorporate all essential features of the kinetics. Elsewhere, we explore the effect of processes specific to the individual systems.[12] In the H+OCS system for example, the unusually high relaxation rate of vibrationally excited CO in OCS ($P\approx 0.1$ for CO(v=4)) must be considered. Inclusion of additional processes in the model of course improves the fit. In no case will any of these secondary processes change the $t\to 0$ limit, but they may influence the time interval over which the linear approximation is valid. Though relaxation rates may in some cases be significant, even gas kinetic, we note that our absorption measurements are sensitive to net changes in population. Net population changes will be small initially, especially near the peak of the distribution, since the relaxation rates into and out of a given state will be comparable. Thus the distributions reported here may reflect some relaxation, but not enough to change any major conclusions.

The validity of the model is supported by the plot in Fig. 2 which is derived from H+OCS data. Multi-parameter iterative fitting can produce ambiguous results, but certain features of the transient signals, such as the time to peak amplitude, are not subject to misinterpretation. For CO(v=0,J=35), $k_{3'}\approx 0$ since this level falls on the tail of the v=0 rotational distribution. In this instance the model predicts an inverse pressure dependence for the time required to reach maximum amplitude, which the plot in Fig. 2 verifies. The time constants derived from iterative fitting also show the predicted pressure dependencies.[12b,c]

The time-resolved absorption technique used in our experiments is not as sensitive as MPI or LIF, but it does present one advantage. Distinction between gain and absorption clearly indicates the presence of population inversion. Thus we are assured, at least qualitatively, of the accuracy of our distributions. The possibility of gain raises an important point. Absorption techniques measure population differences. This means that the initial slope of the absorption signal is proportional to the difference of the upper and lower state specific rate constants. By probing successively higher vibrational levels until no further absorption is observed, the nascent rotational distribution of the highest populated vibrational level is directly determined. Working backwards, the difference measurements yield the distributions in lower vibrational levels. It is important to make these corrections, particularly for H+OCS where excitation of CO is observed up to v=4.

Using the initial slope method, CO rotational and vibrational distributions were determined for the title reactions. Distributions for $H+CO_2$ are shown in Fig. 3, while those for H+OCS are summarized in Table I.

The surprisal analysis procedure developed by Levine, Bernstein, and coworkers[14] was used to compare the observed distributions to statistical distributions based on random sampling of the available phase space. The prior distribution is given by

$$P^{\circ}(v,J) = (2J_{CO}+1) \sum_{v_{XH}=0}^{v^{*}} (1-f_V^{XH}-f_V^{CO}-f_R^{CO})^{\frac{3}{2}}$$

where the V and R subscripts refer to vibration and rotation, f is the fraction of available energy in the designated degree of freedom, and v^* is the highest energetically accessible vibrational level of the HX fragment. Here we assume continuous functions for translation and rotation, and count vibrations explicitly.[12b] The insets in Fig. 3 show rotational surprisal plots for CO(v=0,1) from H+CO_2. The solid lines overlying the rotational distributions represent back-calculated distributions derived from the surprisal analysis. The surprisal parameters listed in Table I summarize the H+OCS results.

Time-resolved sub-Doppler lineshape measurements on the CO(v=0) product from H+OCS indicate substantial partitioning of energy into CM translation. A total of six transitions from J=7 to J=30 were examined: R(7), P(10), R(16), R(19), R(22), and R(30). A 3D plot for R(19) is shown in Fig. 4. Cross sections at 100 ns intervals were fit to Gaussian lineshapes, from which E_{CM} was determined. Since the S/N ratio is initially poor due to the small amount of product present, a preliminary estimation of the nascent E_{CM} was made by fitting a plot of E_{CM} vs time to an exponential function, and extrapolating back to t=0. Such a plot for R(19) is shown in Fig. 4. In all cases the exponential fit appears to have underestimated the nascent CM kinetic energy. We take the average E_{CM} thus determined, 7180 cm^{-1}, as a lower limit for CO(v=0).

4. DISCUSSION

Because of the large difference in mass, it is unlikely that the H atom will simply abstract an O or S atom in passing. While the required slowing of the H atom implies the existence of an intermediate, it does not guarantee statistical distribution of available energy among product degrees of freedom. In the energy regime of these experiments, ≈10,000 cm^{-1} at the transition state, RRKM estimates of reaction rates are on the order of 10^{13} s^{-1}.[15] Since IVR may not be complete on this time scale, the applicability of statistical theory to these experiments is questionable.

4.1. H+CO_2 → CO+OH

With a total of 10,000 cm^{-1} available to the products, the average energy channeled into CO internal degrees of freedom, 1500 cm^{-1} (15%), is surprisingly small. The v=0 and 1 rotational distributions are colder than would be predicted statistically, with rotational surprisal parameters of Θ_R=7 and 9, respectively.

Likewise, our measured vibrational distribution is cold with a [v=1]/[v=0] ratio of 0.4. No signal was detected for 3←2 transitions. We conclude that little or no population of v>1 occurs since it is unlikely that the v=1 and 2 populations are equal.

Our results are consistent with those of Weston and coworkers,[16] but disagree with the study of Rice et al. who found a [v=1]/[v=0] ratio of 1.7 Using VUV LIF, Rice et al. also reported an inverted v=1 rotational distribution peaked at J=23 which should have manifested itself as gain in our experiments: none was observed. While our observations do not quantitatively support those of Rice et al., we both conclude that CO internal excitation is less than statistical.

Previous studies of nascent OH distributions have shown that they too are colder than statistical.[2-4] Using 193 nm photolysis of HBr as the H atom source, an average OH(v=0) rotational energy of 1350 cm^{-1} was determined.[4] Under similar conditions, Chen et al. were able to measure a CM kinetic energy of ≈9800

cm^{-1} for OH(v=0, low J) using sub-Doppler techniques.[17] Although the average energy partitioned into CM translation will be less than 9800 cm^{-1}, all results indicate a propensity for CM translation at the expense of product internal excitation.

Some insight into the dynamics can be gained by examining the HOCO potential energy surface. H and O atom energy contours were generated from analytic functions fit to the surface of Schatz et al..[8] For CO_2 in its equilibrium geometry, a shallow H atom well exists along a C_{2v} approach to the C atom. As the CO_2 molecule is bent and stretched, prominent minima develop in both the cis and trans positions. The geometry shown in Fig. 5 produces the minimum H atom barrier, which is found along a cis approach of the H atom. However, those collisions leading to the distortion of the CO_2 equilibrium geometry shown in Fig. 5 will leave the H atom in the trans position. The resulting dynamical barrier is consistent with the low reaction probability of 0.024 for E_{CM}=2.4 eV,[16] and the strong dependence of reaction probability on collision energy.[12a,17] Similar contours, generated by fixing the H atom at the minima shown in Fig. 5 and moving the O atom, reveal steep gradients forcing the O atom away from the CO.

Evidence for the role of a HOCO intermediate can be found in the oriented precursor work of Zewail and coworkers.[6] They demonstrate that the appearance of OH following photoexcitation of CO_2-HI complexes is delayed by several picoseconds. Insofar as these experiments can be interpreted in terms of $H+CO_2$ collisions, they demonstrate the importance of a HOCO intermediate. But in this case the effect of the nearby halogen atom on reaction mechanism remains to be established.

4.2. H+OCS → CO+SH

Although the energy in the transition state, 9700 cm^{-1}, is comparable to that for $H+CO_2$, the total amount available to the products, 15,000 cm^{-1}, is much greater due to a substantial reaction exothermicity of 11.3 kcal mol^{-1}. It is not surprising, then, to find significantly more internal excitation of the CO product, 1920 cm^{-1} (13%), with measurable population in levels up to v=4. Comparison with statistical theory, however, again indicates a strong bias against channeling of energy into CO internal excitation. The distribution of population over vibrational levels is somewhat cold (Boltzmann temperature of 3890 K) with a vibrational surprisal parameter Θ_V=3.6. The rotational surprisal parameters Θ_R offer a striking comparison, increasing monotonically from 12.9 for v=0 to >50 for v=4 (Boltzmann temperatures from 1400 K down to 175 K). The strong dependence of rotational temperature on vibrational quantum number suggests that CO internal excitation is conserved, that is vibrational excitation occurs at the expense of rotational excitation.

In contrast to OH, predissociation precludes the use of LIF for monitoring the SH fragment. However, the technique has been successfully applied to the SD(v=0,1) product following 193 nm photolysis of DBr.[11] Though the results are not directly comparable to the present studies due to the large difference in available energy, 23,000 cm^{-1} vs 15,000 cm^{-1}, the SD rotational distributions were cold and non-statistical in nature.

Our CO(v=0) transient lineshape measurements for six rotational levels between J=7 and 30 yield an average nascent CM translational energy of 7180 cm^{-1}. This value is an upper limit in that S/N limitations prevented similar measurements over the entire ensemble of CO states, i.e. v>0. Nevertheless, it again underscores preferential partitioning of available energy into CM translation at high collision energies.

Conservation of energy leaves a minimum of 5,900 cm^{-1} for SH internal excitation. To the extent that the D+OCS experiments mentioned earlier are relevant, we can expect that most of this energy will appear as product vibration. Intuitively, this is not surprising since the HS bond undergoes a large change in amplitude during the reactive scattering process.

For H+OCS, there is no potential energy surface to aid in the elucidation of reaction mechanism. Fortunately, the results of our experiments provide a number of clues. We begin by considering CO vibrational excitation. Mapping of OCS ν_1 (C-O stretch) harmonic oscillator wave functions onto those of the free CO molecule produces a vibrational distribution of only 1020 K. Hence a simple Franck-Condon analysis based upon a sudden crossing from the OCS to the CO surface will not suffice to explain the observed 3890 K CO

vibrational distribution. Energy must be coupled into the CO stretch of the HSCO intermediate during the reaction.

Assuming a short-lived HSCO intermediate (incomplete IVR), two limiting approach geometries present themselves, side-on and end-on. For side-on approach of the H atom, little excitation of the CO stretch would be expected since the force of the collision is directed along an axis normal to the C-O bond. In addition, large impact parameters expected with side-on collisions would introduce substantial orbital angular momentum, which should be conserved as product rotation. In contrast for collinear approach, compression of the S-C and C-O bonds would serve to slow the H atom, ultimately resulting in some CO vibrational excitation. The small impact parameter inherent in the collinear geometry also predisposes the products to little rotational excitation. We conclude that our experiments suggest a collinear geometry in the reactive process.

We note in closing the work of Flynn and coworkers who reached similar conclusions in their inelastic H+OCS scattering studies.[18] They found a negative correlation between vibrational and rotational excitation. Those collisions which produced excitation of the OCS ν_1 mode caused statistically little rotational excitation.

5. CONCLUSION

We have studied reactive scattering of H atoms with CO_2 and OCS at $\approx 10{,}000$ cm^{-1} above the barrier through state resolved monitoring of the CO product. The CO rotational and vibrational distributions obtained under arrested relaxation conditions are significantly colder than those predicted by statistical theory. Our results, coupled with earlier studies, indicate incomplete
IVR in the HOCO and HSCO intermediates, with preferential partitioning of available energy into CM frame translational degrees of freedom.

6. ACKNOWLEDGEMENT

H.E.C. wishes to thank the Flynn Group for their assistance. In particular, helpful discussion of the data with George Flynn, suggestions concerning experimental technique from Tom Kreutz, and the use of John Herschberger's line search program proved invaluable.

This work was supported by the Army Research Office and the Office of Naval Research.

7. REFERENCES

1. C.R. Quick and J.J. Tiee, Chem. Phys. Lett. 100, 223 (9183).

2. K. Kleinermanns, E. Linnebach, and J. Wolfrum, J. Phys. Chem. 89, 2525 (1985).

3. A. Jacobs, M. Wahl, R. Weller, and J. Wolfrum, Chem. Phys. Lett. 158, 161 (1989).

4. G. Radhakrishnan, S. Buelow, and C. Wittig, J. Chem. Phys. 84, 727 (1986).

5. J. Rice, G. Hoffman, and C. Wittig, J. Chem. Phys. 88, 2841 (1988).

6. N.F. Scherer, L.R. Khundkar, R.B. Bernstein, and A.H. Zewail, J. Chem. Phys. 92, 5239 (1990).

7. (a) J.K. Rice, Y.C. Chung, and A.P. Baronavski, Chem. Phys. Lett. 167, 151 (1990); (b) J.K. Rice and A.P. Baronavski, J. Chem. Phys. 94, 1006 (1991).

8. G.C. Schatz, M.S. Fitzcharles, and L.B. Harding, Faraday Disc. Chem. Soc. 84, 359 (1987).

9. S. Tsunashina, T. Yokota, I. Safarik, H.E. Gunning, and O.P. Strausz, J. Phys. Chem. 79, 775 (1975).

10. J.H. Lee, L.J. Stief, and R.B. Timmons, J. Chem. Phys. 67, 1705 (1977).

11. D. Hauesler, J. Rice, and C. Wittig, J. Chem. Phys. 91, 5413 (1987).

12. (a) S.L. Nickolaisen, H.E. Cartland, and C. Wittig, J. Chem. Phys., submitted for publication; (b) S.L. Nickolaisen, PhD dissertation, University of Southern California (1991); (c) S.L. Nickolaisen and H.E. Cartland, J. Chem. Phys., in preparation.

13. H. Okabe, Photochemistry of Small Molecules (John Wiley & Sons, New York, 1978) p. 165.

14. R.D. Levine and R.B. Bernstein, Acc. Chem. Res. 7, 393 (1974).

15. G. Hoffman, D. Oh, Y. Chen, and C. Wittig, Israel J. Chem. (1989).

16. R.E. Weston, private communication.

17. Y. Chen, G. Hoffman, D. Oh, and C. Wittig, Chem. Phys. Lett. 159, 426 (1989).

18. L. Zhu, J.F. Hershberger, and G.W. Flynn, J. Chem. Phys. 92, 1687 (1990).

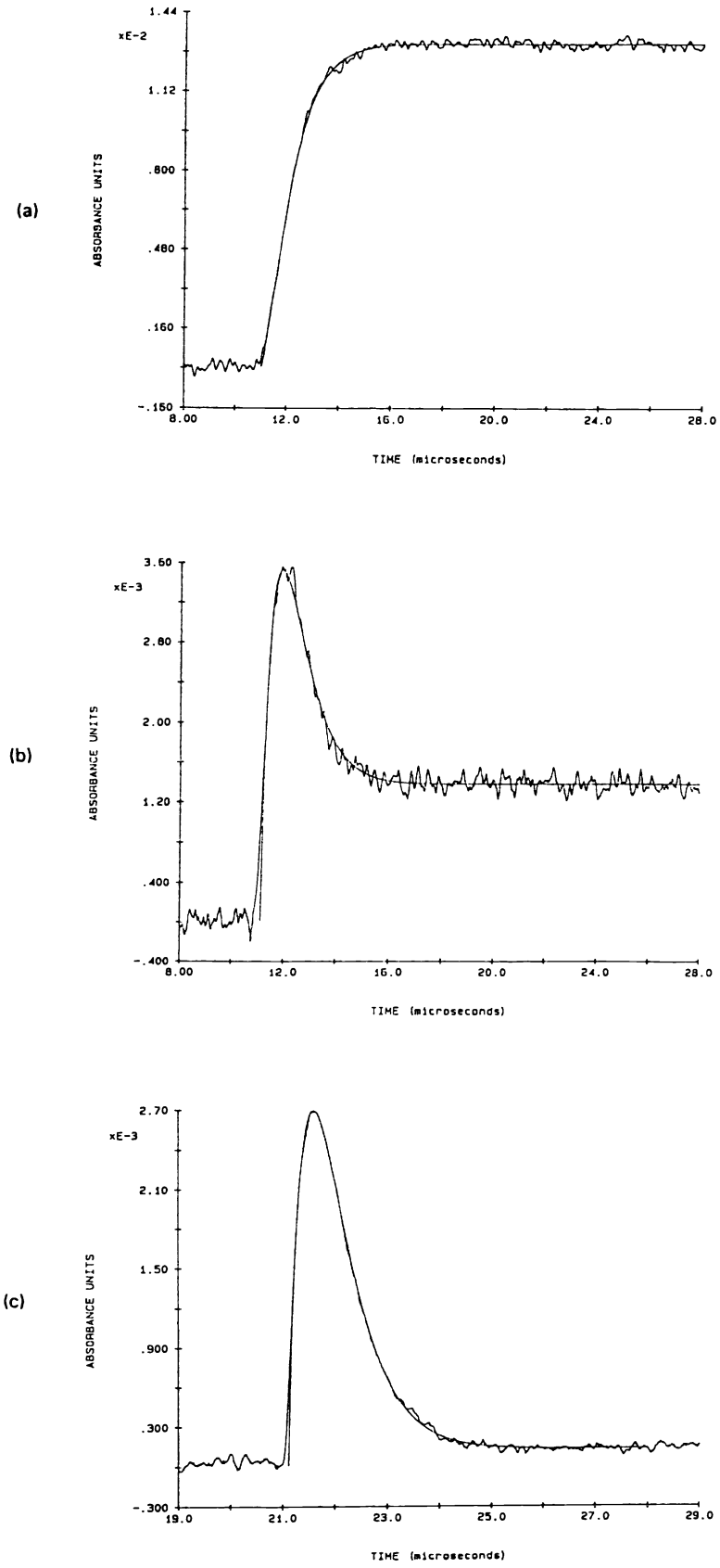

Figure 1. CO(v = 0) transient absorption signals from H + OCS→CO + SH; (a) P(10), (b) R(20), (c) P(35).

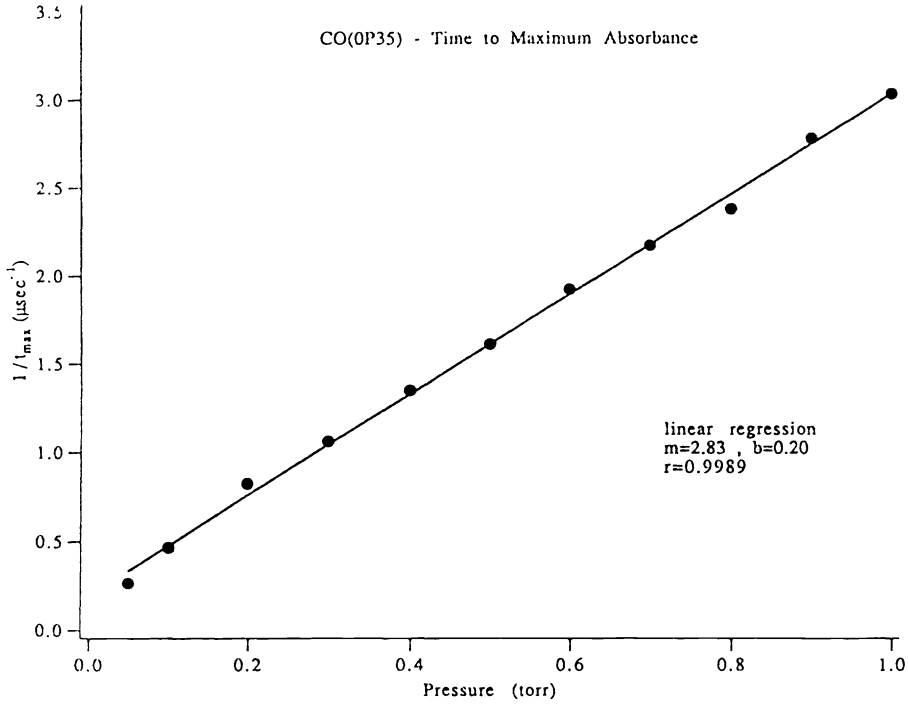

Figure 2. The time to maximum signal amplitude for CO(v = 0,J = 35) from H + OCS→CO + SH shows the pressure dependence predicted by the model.

Table I. Nascent CO product rotational temperatures T_R and surprisal parameters Θ_R from H + OCS→CO + SH. The vibrational temperature $T_V = 3890 \pm 830$ K and surprisal parameter $\Theta_V = 3.6 \pm 1.1$.

CO vibrational quantum number	Boltzmann temperature T_R (K)	Surprisal parameter Θ_R
0	1400 ± 140	12.9 ± 1.4
1	780 ± 45	21.3 ± 1.3
2	590 ± 100	24.0 ± 3.8
3	405 ± 20	28.6 ± 1.5
4	175 ± 20	51.9 ± 5.6

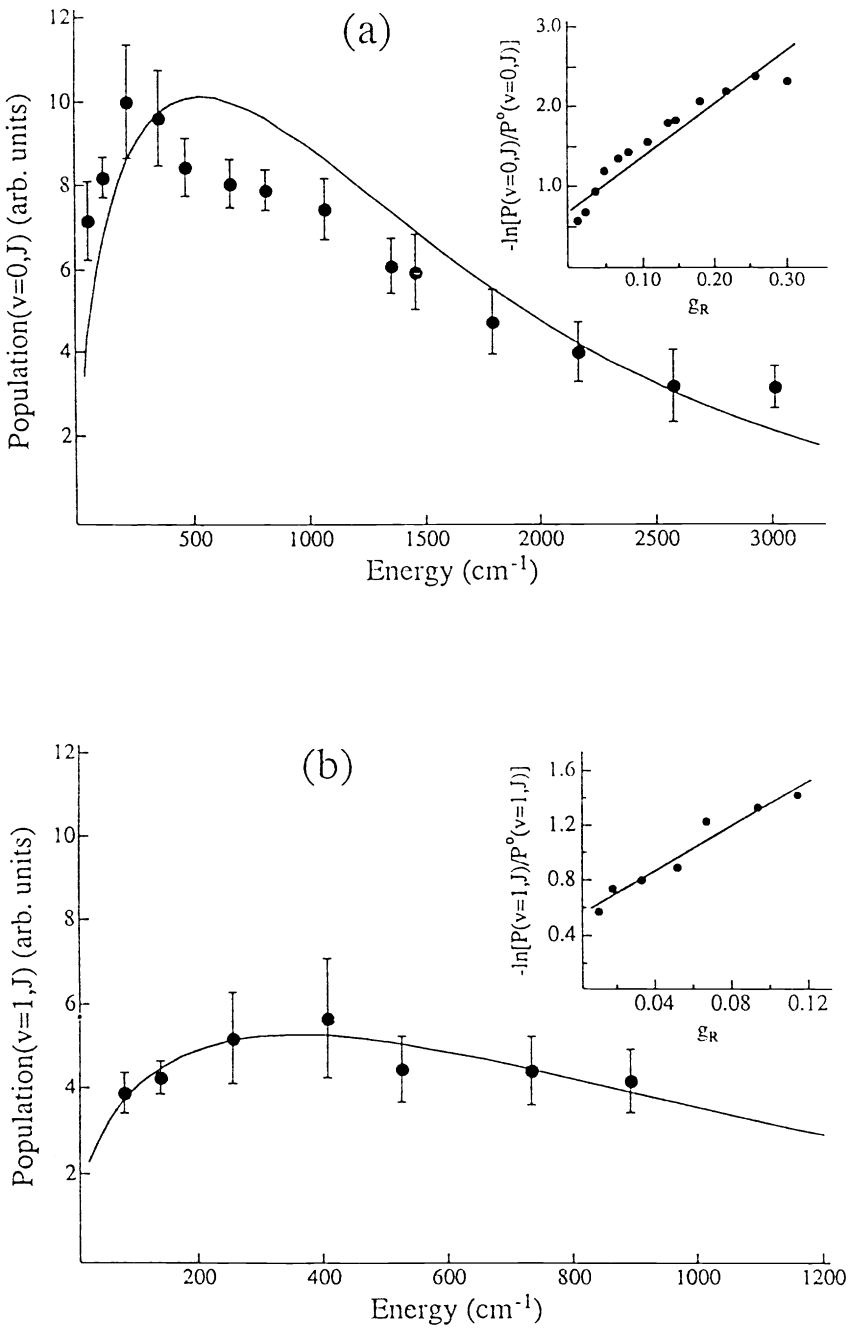

Figure 3. CO rotational distributions from $H + CO_2 + CO + OH$; (a) $v = 0$, (b) $v = 1$. Solid lines are from surprisal analyses (insets); $\Theta_R = 7$ and 9 for $v = 0$ and 1, respectively.

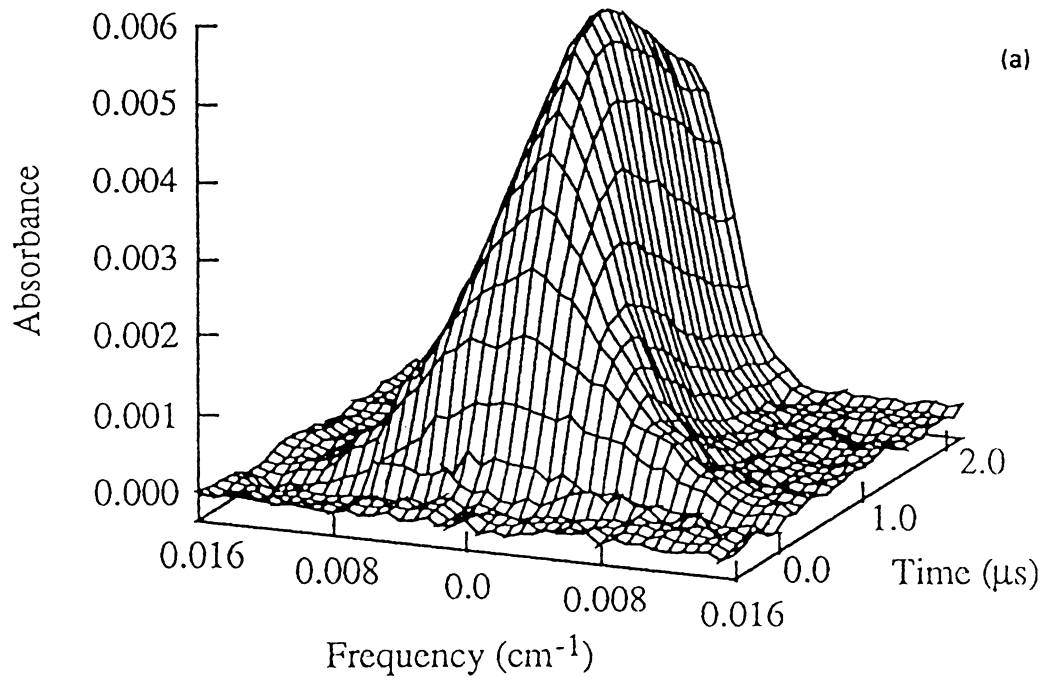

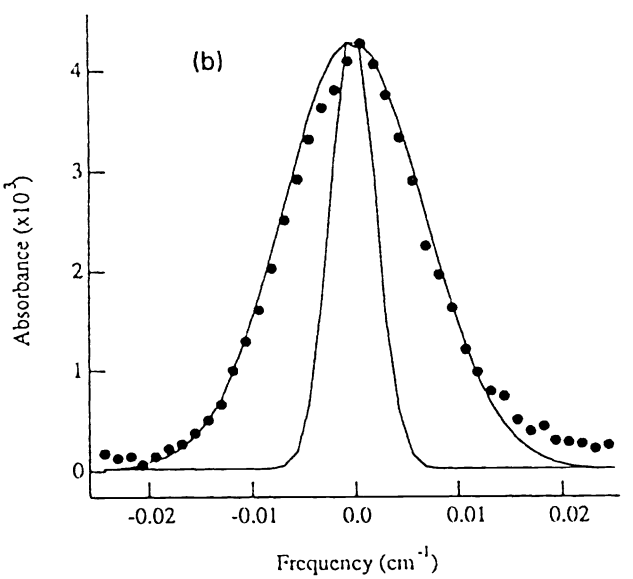

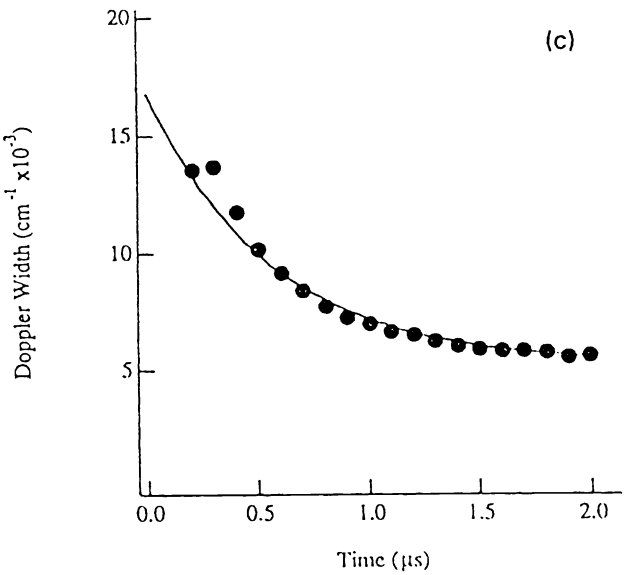

Figure 4. Time-resolved sub-Doppler spectroscopy of CO(v=0, R19) from H+OCS→CO+SH; (a) absorbance as a function of frequency and time, (b) lineshape, Gaussian fit, and 298 K reference lineshape at 500 ns following the photolysis pulse, (c) Doppler width versus time extrapolates to 0.0168 cm^{-1} at t=0.

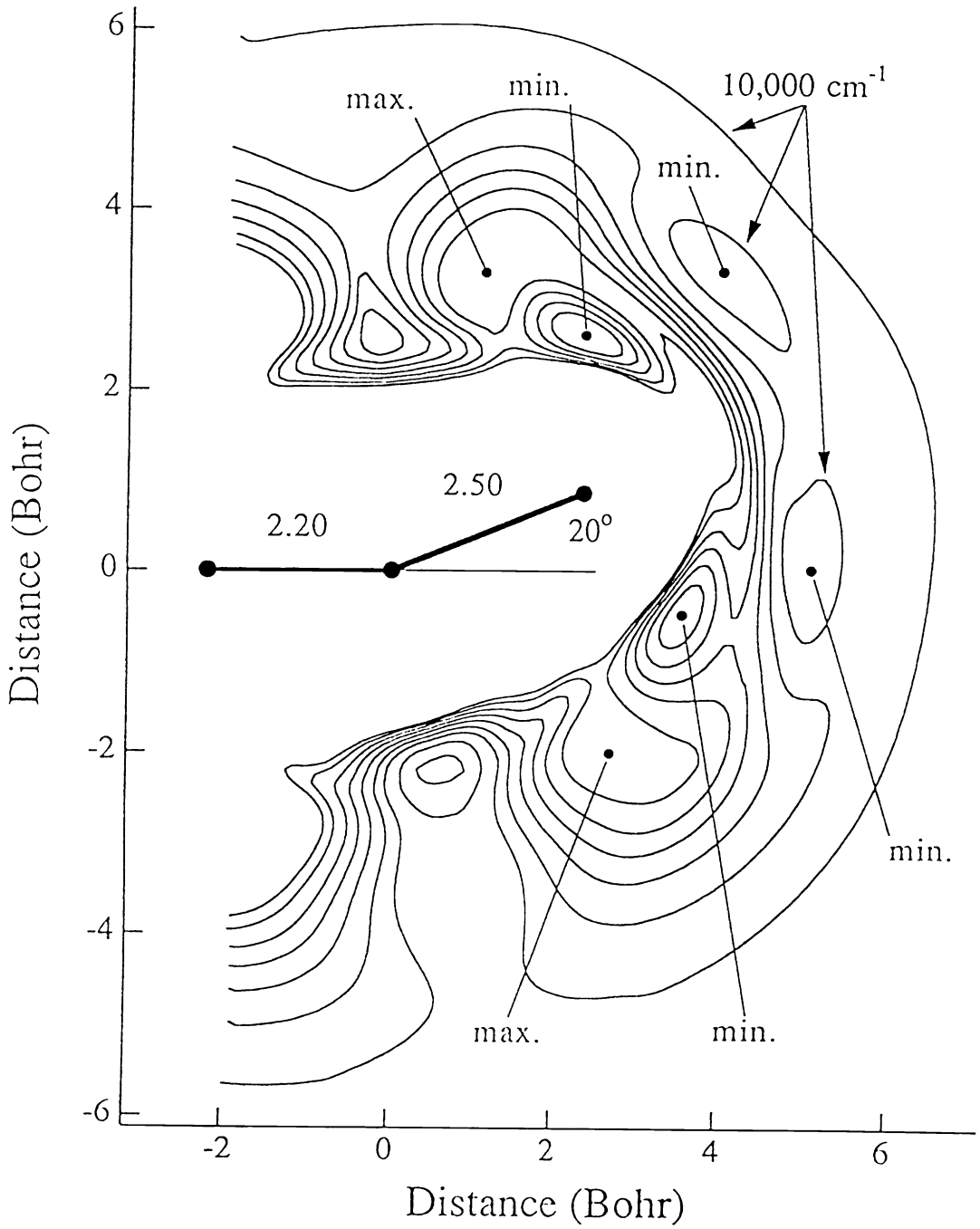

Figure 5. H atom energy contours for $H+CO_2$ at the cis saddle point geometry. Contours are separated by 2500 cm^{-1}; the highest is at 25,000 cm^{-1}.